

Geometry versus Entanglement in Resonating Valence Bond Liquids

Himadri Shekhar Dhar¹ and Aditi Sen(De)^{2,1}

¹*School of Physical Sciences, Jawaharlal Nehru University, New Delhi 110067, India*

²*Harish-Chandra Research Institute, Chhatnag Road, Jhansi, Allahabad 211019, India*

We investigate the behavior of bipartite as well as genuine multipartite entanglement of a resonating valence bond state on a ladder. We show that the system possesses significant amounts of bipartite entanglement in the steps of the ladder while no substantial bipartite entanglement is present in the rails. Genuine multipartite entanglement present in the system is negligible. The results are in stark contrast with the entanglement properties of the same state on isotropic lattices in two and higher dimensions, indicating that the geometry of the lattice can have important implications on the quality of quantum information and other tasks that can be performed by using multiparty states on that lattice.

I. INTRODUCTION

Resonating valence bond (RVB) states were introduced in 1938 by Pauling in organic, and later in metals and intermetallic, compounds [1]. It was extensively studied in many body physics ever since Anderson, in 1973, presented the idea of using such states to explain the behavior of Mott insulators [2]. The importance of RVB states grew immensely after the proposition of relating such states with high temperature superconductivity [3, 4]. Investigations on the use of RVB states in quantum information has been initiated in recent years. The possibility of topological quantum computation by using such states have been proposed [5], and the entanglement properties of RVB states in isotropic two- and three-dimensional lattices have also been explored [6].

In this paper, we consider the RVB state on a ladder, a pseudo two-dimensional system (See Fig. 1). Ladder

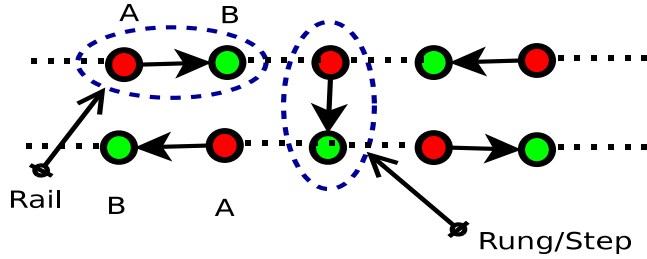


FIG. 1: (Color online.) RVB liquid on a ladder. Blue and Red balls belong to two different sublattices A and B respectively. One particular dimer covering is shown. Singlets are always from sublattice A to sublattice B .

states (obtained by assembling spin chains one next to the other to form *ladders* of increasing width) have recently generated a lot of interest in theoretical and experimental condensed matter physics. Ladder states have been proposed in the study of superconductivity in systems like doped $(VO)_2P_2O_7$ [7] and the study of transitions from 1-D chains to 2-D spin systems [8]. It has been found that ground states of antiferromagnetic Heisenberg models (with suitable couplings) on “even ladders” (consisting of two or more even number of chains) can be RVB

states [8–10]. Quantum information concepts like entanglement, fidelity, of different ladder systems have been studied [11], and protocols for high fidelity transmission of quantum states through such systems have also been presented [12].

Main results

We study the entanglement properties of RVB states on a pseudo-two dimensional ladder. Precisely, we consider ladders of two chains ($2 \times M$ ladders, $N=2M$ spins), of different lengths. We find that the entanglement characteristics of an RVB state on a ladder are significantly different from that on an isotropic two or higher dimensional lattice. Bipartite entanglement between neighboring sites are of two different types for the case of a ladder. While the bipartite entanglement of the neighboring sites on the rails of the ladder is insignificant, that of the steps (or rungs) is substantial. This automatically suggests that genuine multipartite entanglement of the ladder RVB is negligible. This is in sharp contrast with the situation on an isotropic 2D or 3D lattice, where the single type of nearest neighbor bipartite entanglement is negligible, while the state is genuine multipartite entangled [6]. We reach our conclusions by numerical simulations as well as via analytical bounds on the entanglement measures. The symmetry of the system leads us to use the singlet fraction as a measure of bipartite entanglement, while in the multipartite case, we use a recently proposed measure called “generalized geometric measure” [13, 14].

This change in the entanglement properties can be attributed to the change in the geometry of the RVB system: a ladder is not isotropic in all directions. Our results show that this change in geometry has a marked effect on the entanglement properties of the system, and hence on quantum information tasks possible. The results are obtained by using periodic boundary conditions. However, we have also found the similar trend of bipartite entanglement, when there is open periodic boundary condition. Also the calculations were done for the, physically interesting, so-called RVB liquid, which we now define.

II. RVB LIQUID

The pseudo two-dimensional lattice under consideration can be divided into sub-lattices (see Fig. 1), A and B, in such a way that all the nearest neighbor (NN) sites of any site on sub-lattice A belong to sub-lattice B, and vice-versa. Such a lattice is called a *bipartite lattice*. Each lattice site on such a bipartite ladder is occupied by a qubit, which can for example be the spin state of an electron. For such a system, the RVB state is defined as the equal superposition of all the possible dimer (singlet) coverings that can be formed by nearest-neighbor *directed* dimers. Between site i in sublattice A and site j in sublattice B, a directed dimer is defined as

$$|(i, j)\rangle = \frac{1}{\sqrt{2}}(|\uparrow_i\downarrow_j\rangle - |\downarrow_i\uparrow_j\rangle),$$

where $|\uparrow\rangle$ and $|\downarrow\rangle$ are respectively the spin-up and spin-down states in the z -direction, at the corresponding lattice site. The (unnormalized) RVB state can then be written as [15]

$$|\psi\rangle = \sum |(a_1, b_1)(a_2, b_2)\dots(a_N, b_N)\rangle, \quad (1)$$

where a_i and b_j are site positions and the summation is over all dimer coverings such that the dimers in every covering satisfy $a_i \in A$ and $b_j \in B$. Since the dimer coverings that constitute the RVB state are formed by using only NN dimers, we call the state $|\psi\rangle$ as an *RVB liquid*.

III. BIPARTITE ENTANGLEMENT OF RVB LIQUID

We are now ready to study the behavior of nearest-neighbor bipartite states for an RVB liquid on a ladder. To obtain the bipartite density matrix, ρ_{12} , between any site (say, 1) in A and one of its nearest neighbors (say, 2) in B, we take the partial trace of the whole RVB liquid over all sites except 1 and 2:

$$\rho_{12} = \text{Tr}_{\overline{12}} |\psi\rangle \langle\psi| \quad (2)$$

where $\text{Tr}_{\overline{12}}$ represents the partial trace over all sites other than 1 and 2. Rotational invariance of $|\psi\rangle$, given in Eq. (1), implies that ρ_{12} (and all other reduced density matrices of $|\psi\rangle$) is also rotationally invariant. The only rotationally invariant two-qubit states are the singlet and the maximally mixed state. Therefore, ρ_{12} is the Werner state [16] given by

$$\rho_{12}(p) = p |(i, j)\rangle \langle(i, j)| + \frac{1-p}{4} I_4, \quad (3)$$

where the ‘‘Werner parameter’’ p satisfies $-1/3 \leq p \leq 1$, and I_4 is the identity operator of the four-dimensional complex Hilbert space. Bipartite entanglement measures, like concurrence [17], are monotonic functions of p .

Hence, instead of calculating entanglement measures explicitly, we will investigate the behavior of p with respect to increase of system size. Note here that the Werner state is entangled for $p > 1/3$.

A. Properties of nearest-neighbor bipartite states for periodic boundary conditions

In this subsection, we will investigate the bipartite entanglement of two neighboring sites of the ladder with periodic boundary conditions.

1. Bipartite Entanglement: Steps versus Rails

As mentioned earlier, the nearest-neighbor bipartite state of the RVB liquid is a Werner state. By symmetry, there are only two types of such bipartite states: along any one of the rails, and on a step. We denote the Werner parameter p of a Werner state along a rail as p_r , while that on a step as p_s (see Fig. 1).

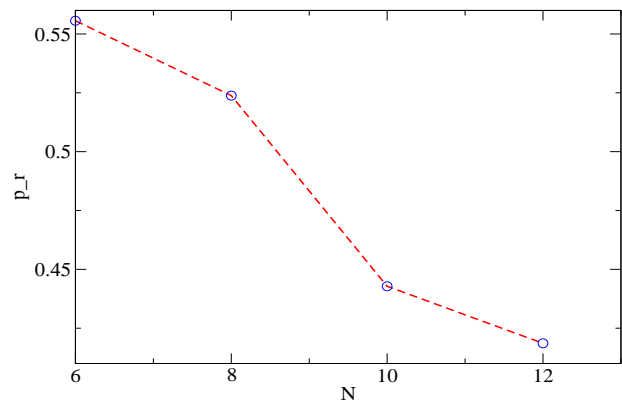


FIG. 2: (Color online.) Bipartite entanglement on the rails. The decrease of the entanglement parameter p_r with increasing N is clearly seen.

As shown in Fig. 2, the values of p_r consistently decrease with the increasing system size N , and hence bipartite entanglement on the rails decreases with the increasing N , similar to the case of an isotropic lattice. Interestingly, however, the BE of the steps *increases* with respect to N (see Fig. 3).

Therefore, already at the level of bipartite entanglement, one obtains a trade-off between the two different forms of nearest-neighbor entanglement, in the case of an RVB liquid on a ladder. Contrast this with the case of a square lattice or any other isotropic lattice, where the corresponding RVB liquids have only a single type of nearest-neighbor entanglement, and its value, quite generally, decreases with increasing system size [6]. The numerical evidence presented above for this complementary

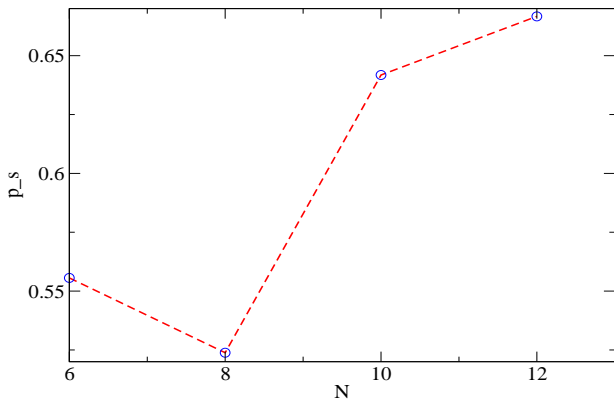


FIG. 3: (Color online.) Bipartite entanglement on the steps. In sharp contrast to the isotropic case, bipartite entanglement on the steps, as parametrized by p_s , increases with increasing system size N .

behavior of the two types of BE, present in the ladder, will later in the paper also be justified by using analytic bounds.

2. Regional Entanglement

To study the behavior of BE between nearest neighbors, we introduce a quantity, called “regional entanglement” (denoted as p_{avg}) for each lattice site. For every lattice site, there are three NN sites, which form three nearest-neighbor bipartite entanglements with that site. (Note that we are still in the regime of periodic boundary conditions.) Regional entanglement at a particular site is defined as the average of these three nearest-neighbor entanglements, as quantified by their Werner parameters. Due to periodic boundary conditions, the regional entanglement at each site is the same, so that it is a characteristic parameter for a given ladder lattice size. It is a measure of the regional distribution of bipartite entanglement at any lattice site.

The physical significance of p_{avg} can be understood by using the concept of *fidelity of teleportation* [18, 19]. Suppose that an arbitrary two-dimensional quantum state is available near a particular lattice site, and the task is to quantum teleport [18] the state to a neighboring lattice site, say the one on the other rail. The fidelity of teleportation for such an exercise is given by [19]

$$F_{tele}^s = \frac{p_s + 1}{2}.$$

However, the same protocol that teleports the quantum state to the NN site on the other rail, will also teleport the state, with a different teleportation fidelity, to two other NN sites on the same rail [19], with the new fidelity being

$$F_{tele}^r = \frac{p_r + 1}{2}.$$

The average fidelity of the transfer is given by

$$F_{tele} = \frac{2F_{tele}^r + F_{tele}^s}{3} = \frac{p_{avg} + 1}{2}. \quad (4)$$

Numerical simulations show that although there are two types of bipartite entanglement, which show complementary behavior with increasing system size, the regional entanglement, p_{avg} , decreases as the size of the lattice is increased (see Fig. 4).

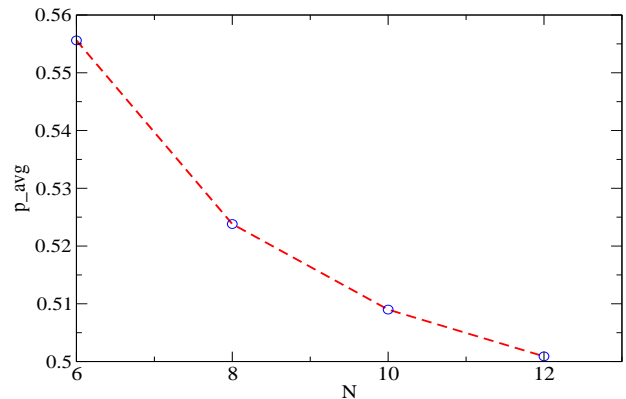


FIG. 4: (Color online.) Regional entanglement in RVB liquids on ladders of different sizes.

To sum up, regional entanglement of RVB liquid on ladders is a quantity that mirrors the behavior of nearest-neighbor bipartite entanglement of isotropic lattice RVBs. However, the internal picture of bipartite entanglement in RVBs is far richer and depends on the geometry of the lattice. We have also observed that in the case of RVB ladders without periodic boundary conditions, the complementary behavior between bipartite entanglement of rails and steps remains the same as in the case of ladders with periodic boundary conditions.

B. Analytical estimates of bipartite entanglement

1. Upper Bounds from Monogamy of Entanglement

A first estimate on the bipartite entanglement can be obtained by using monogamy of entanglement [20]. Let us consider an arbitrary site i_A , say on sublattice A . If the lattice is finite, and if periodic boundary conditions are not assumed, we assume that i_A is not on a boundary step (see Fig. 1). Each such site is surrounded by three NN sites, belonging to the sublattice B . Rotational invariance of the state $|\psi\rangle$ ensures that all the three NN bipartite states are in Werner states, of which two have Werner parameter p_r , and one has p_s . The monogamy of entanglement [20] demands that $2\tau(\rho_r) + \tau(\rho_s) \leq \tau_{1:\text{rest}}(|\psi\rangle)$. $\tau(\rho)$ is the “tangle” of the bipartite state ρ , and is defined as $\max(0, \lambda_1 - \lambda_2 - \lambda_3 - \lambda_4)$, where

λ_i 's are the square roots of the eigenvalues, in decreasing order, of $\rho\tilde{\rho}$. Here, $\tilde{\rho} = (\sigma_y \otimes \sigma_y)\rho^*(\sigma_y \otimes \sigma_y)$, where complex conjugation is with respect to the σ_z eigenbasis [17, 20]. And $\tau_{1:\text{rest}}(|\psi\rangle)$ is the tangle of the state $|\psi\rangle$ in any bipartition of one site to rest of the sites, and is unity. Also $\tau(\rho(p_{r/s})) = (3p_{r/s} - 1)^2/4$, so that the monogamy inequality reads

$$(3p_r - 1)^2/2 + (3p_s - 1)^2/4 \leq 1, \quad (5)$$

The bound on p_r and p_s obtained in the form of the above inequality is depicted in Fig. 5. The 2D projection of Fig. 5 clearly shows that the allowed value for p_s can go up to 1 while the same for p_r is ≤ 0.8 . Therefore, the complementary behavior between the entanglements in the rails and steps can also be anticipated from the monogamy inequality.

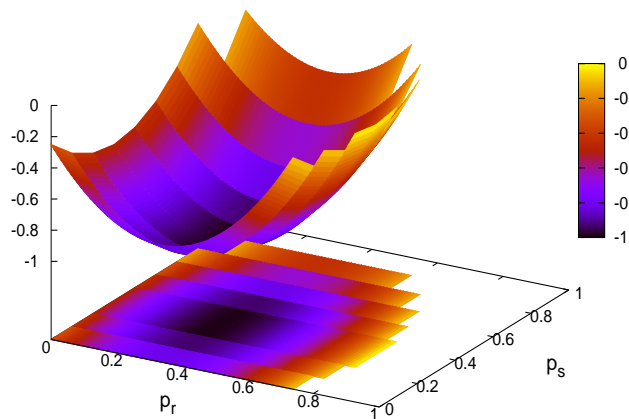


FIG. 5: (Color online.) Estimate of Werner parameters from the monogamy of entanglement. The allowed combinations of p_r and p_s are those for which the surface $(3p_r - 1)^2/2 + (3p_s - 1)^2/4 - 1$ is negative, and can be read off from the projection of the surface.

2. Bounds from Asymmetric Cloning

Consider again the task of sending an arbitrary auxiliary qubit from any site i_A to its three neighboring sites [18]. The teleportation fidelity of the output state at a site on the same rail (as i_A) will be $(p_r + 1)/2$, while the fidelity will be $(p_s + 1)/2$ of the output state on the other rail [19]. Quantum mechanics implies that the fidelities of the output states in the whole protocol cannot exceed the fidelities of three approximate clones of the initial state in the optimal $1 \rightarrow (1 + 2)$ asymmetric quantum cloning machine [21, 22]). Therefore, we obtain

$$p_r \leq \frac{1}{3}(\sin^2 \theta + \sqrt{2} \sin 2\theta); \quad p_s \leq 1 - \frac{4}{3} \sin^2 \theta, \quad (6)$$

for all possible θ . Note here that if $\theta \rightarrow 0$, it would imply $p_r \leq 0$ and $p_s \leq 1$. Moreover, $p_r \leq 0$ will imply no bipartite entanglement in the rails while there can be some – in principle, maximal – entanglement in the steps. Numerical evidence (in Figs. 2 and 3) also suggest that this is indeed the trend of p_r and p_s . In case of a multipartite state, maximal bipartite entanglement in any of its two-party reduced density matrices leads to no genuine multipartite entanglement. The question remains whether θ will be zero for large system-size.

To obtain estimates of θ , we insert the values of p_r and p_s , that have been obtained from the numerical simulations (for different N) in Sec. IIIA, in the inequalities in (6). We then solve the above inequalities to obtain $\theta \in S_1^N$ for the first inequality for a fixed N , and similarly $\theta \in S_2^N$. We now consider the allowed θ lying in the intersection $S_1^N \cap S_2^N$, and plot $\theta_{\max} = \max\{\theta : \theta \in S_1^N \cap S_2^N\}$ with respect to N . We find that θ_{\max} is decreasing with

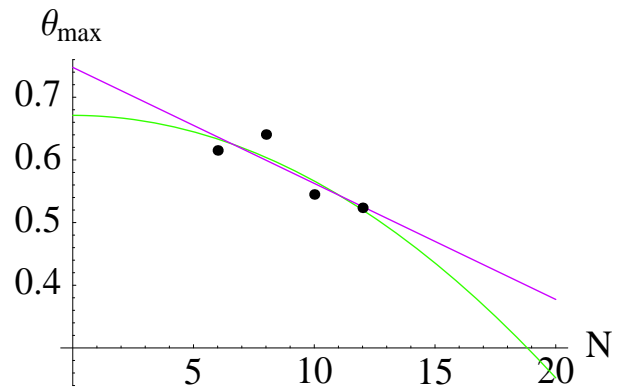


FIG. 6: (Color online.) Decrease of θ_{\max} for increasing N . The dots represent θ_{\max} obtained from Eq. (6) corresponding to $N = 6, 8, 10, 12$. Pink and green lines are respectively linear ($0.747664 - 0.0185155x$) and quadratic ($0.671077 - 0.0010471x^2$) fits of the points. The corresponding mean square errors are 1.22×10^{-3} for the linear fit and 1.06×10^{-3} for the quadratic.

the increase of the size of the lattice, as shown in Fig. 6. The inequalities in Eq. (6) also shows the complementarity between the entanglement of rails and steps (see Fig. 7).

This gives us further evidence that there is negligible or no multipartite entanglement for large lattice size, in contrast to the case of isotropic lattices [6]. We will concretize this evidence by calculating a measure of genuine multipartite entanglement for RVB liquids on ladders, in the next section.

IV. NEGLIGIBLE GENUINE MULTIPARTITE ENTANGLEMENT

The numerical and analytical studies on nearest-neighbor bipartite entanglement in the preceding section

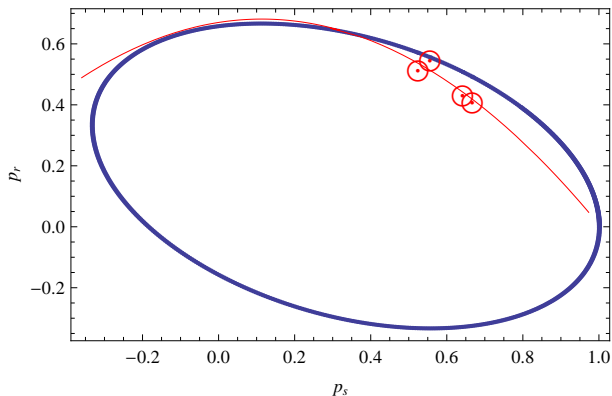


FIG. 7: (Color online.) Complementary behavior of the entanglement on the rail with that on the step. The bound on p_r and p_s , as obtained from the Eq. (6), for all possible values of θ , is depicted by the ellipse in the figure. The allowed combinations of p_r and p_s fall inside the ellipse. The (red) open curve is the quadratic fit ($-0.858x^2 + 0.241x + 0.67$) of the (red) circles, which are in turn the values found by exact calculations for $N = 6, 8, 10, 12$. All calculated points are within the bounding ellipse. It is evident that as p_s attains the maximum value 1, the value of p_r goes to 0.

already suggest that the RVB liquid on a ladder has negligible or no genuine multiparty entanglement. This is due to the evidence presented that the entanglement of the states on the steps are near-maximal or maximal. A maximally entangled state in $d \otimes d$ must be pure [23] (cf. [24]), and hence cannot have any correlation, classical or quantum, with any other quantum system (cf. [25]).

To quantify the amount of genuine multiparty entanglement present in the RVB liquid on ladders of different sizes, we consider a recently introduced genuine multipartite entanglement measure called generalized geometric measure (GGM) [13, 14]. The GGM of an N -party pure quantum state $|\phi_N\rangle$ is defined as

$$\mathcal{E}(|\phi_N\rangle) = 1 - \Lambda_{\max}^2(|\phi_N\rangle), \quad (7)$$

where $\Lambda_{\max}(|\phi_N\rangle) = \max|\langle\chi|\phi_N\rangle|$, with the maximization being over all pure states $|\chi\rangle$ that are not genuinely N -party entangled. It was shown in Ref. [14] that

$$\mathcal{E}(|\phi_N\rangle) = 1 - \max\{\lambda_{A:B}^2 | A \cup B = \{1, 2, \dots, N\}, A \cap B = \emptyset\}. \quad (8)$$

where $\lambda_{A:B}$ is the maximal Schmidt coefficients in the $A : B$ bipartite split of $|\phi_N\rangle$.

In Fig. 8, we find that indeed the genuine multipartite entanglement measure \mathcal{E} for the RVB liquid on a ladder, decreases with increasing N . We also notice that when performing the maximization in Eq. (8) for obtaining the GGM, the maximum Schmidt coefficient is obtained when the maximum number of steps is included on one

side of the bipartition. This can be explained by the complementary behavior of bipartite entanglement in steps and rails as discussed earlier. Therefore, the trend of multipartite as well as bipartite entanglements indicate that for large N , only bipartite entanglement in the steps will remain, while bipartite entanglement of the rails as well as multipartite entanglement of the whole RVB liquid will disappear.

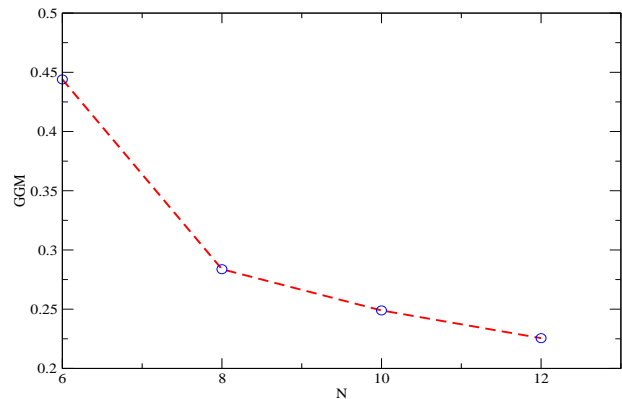


FIG. 8: (Color online.) Genuine multipartite entanglement measure of RVB liquid on ladders. The figure clearly shows that the genuine multipartite entanglement decreases with the increase of system size N .

V. CONCLUSION

We have considered the resonating valence bond liquid on a ladder with periodic boundary conditions. We have found two different kinds of bipartite entanglement: While the bipartite entanglement on the steps is increasing, that of the rails is decreasing, with the increase of the size of the lattice. Both numerical and analytical bounds support this thesis. Moreover, genuine multipartite entanglement of the ladder decreases with increasing system size. This is in sharp contrast with the situation in isotropic lattices, where same state (RVB liquid) has negligible bipartite entanglement, but substantial multipartite entanglement. This shows that geometry can play an important role in determining the entanglement properties of multiparty quantum states.

Acknowledgments

We thank Ujjwal Sen for helpful discussions.

-
- [1] L. Pauling, Proc. R. Soc. London, Ser. A **196**, 343 (1949); L. Pauling, *The Nature of Chemical Bonds* (Cornell University Press, Ithaca, NY, 1960).
- [2] P. Fazekas and P.W. Anderson, Philos. Mag. **30**, 23 (1974).
- [3] P.W. Anderson, Science, **235**, 1196 (1987).
- [4] G. Baskaran, Indian J. Phys. **89**, 583 (2006).
- [5] A. Y. Kitaev, Ann. Phys. (Leipzig) **303**, 2 (2003).
- [6] A. Chandran, D. Kaszlikowski, A. Sen(De), U. Sen, and V. Vedral, Phys. Rev. Lett. **99**, 170502 (2007).
- [7] E. Dagatto, J. Riera and D. Scalapino, Phys. Rev. B **45**, 5744 (1992).
- [8] E. Dagatto and T.M. Rice, Science **271**, 618 (1996).
- [9] S. R. White, R.M. Noack, D. J. Scalapino, Phys. Rev. Lett **73**, 886 (1994).
- [10] G. Sierra and M.A. Martin-Delgado, Phys. Rev. B **56**, 8774 (1997).
- [11] A. Tribedi and I. Bose, Phys. Rev. A **79**, 012331 (2009); I.A. Kovács and F. Iglói, Phys. Rev. B **80**, 214416 (2009), and references therein.
- [12] Y. Li, T. Shi, B. Chen, Z. Song, and C.-P. Sun, Phys. Rev. A **71**, 022301 (2005).
- [13] A. Sen(De) and U. Sen, Phys. Rev. A **81**, 012308 (2010)
- [14] A. Sen(De) and U. Sen, arXiv:1002.1253 [quant-ph]
- [15] S. Liang, B. Doucot, and P.W. Anderson, Phys. Rev. Lett. **61**, 365 (1988).
- [16] R.F. Werner, Phys. Rev. A **40**, 4277 (1989).
- [17] W.K. Wootters, Phys. Rev. Lett. **80**, 2245 (1998).
- [18] C.H. Bennett, G. Brassard, C. Crépeau, R. Jozsa, A. Peres, and W.K. Wootters Phys. Rev. Lett. **70**, 1895 (1993).
- [19] P. Horodecki, M. Horodecki, and R. Horodecki, Phys. Rev. A, **60**, 1888 (1999).
- [20] V. Coffman, J. Kundu, and W.K. Wootters, Phys. Rev. A **61**, 052306 (2000); T.J. Osborne and F. Verstraete, Phys. Rev. Lett. **96**, 220503 (2006).
- [21] M. Murao, D. Jonathan, M.B. Plenio, and V. Vedral, Phys. Rev. A **59**, 156 (1999).
- [22] S. Iblisdir, A. Acín, N.J. Cerf, R. Filip, J. Fiurasek, and N. Gisin, Phys. Rev. A **72**, 042328 (2005).
- [23] Private communication with M. Horodecki, U. Sen, and W.K. Wootters, of one of the authors.
- [24] R. Garisto and L. Hardy, Phys. Rev. A **60**, 827 (1999).
- [25] A. Ekert, Phys. Rev. Lett. **67**, 661 (1991).